Atmospheric Conditions Evaluation for Lucky Imaging at Xinglong Observatory

E Xiang, Kefeng Xu, Yuli Xia
Science and Technology on Integrated Information System Laboratory
Institute of Software Chinese Academy of Sciences
Beijing, China
e-mail: xiange@iscas.ac.cn, kefeng@iscas.ac.cn, yuli@iscas.ac.cn

Huijuan Wang, Xianqun Zeng, Yongna Mao
Key Laboratory of Optical Astronomy
National Astronomical Observatories, Chinese Academy of Sciences
Beijing, China
e-mail: wanghj@nao.cas.cn, zengxq@nao.cas.cn, nymao@nao.cas.cn

***Abstract*—Lucky imaging is a method of high resolution imaging without Adaptive Optics (AO) system, and widespread in astronomy and space target observation. We measured atmospheric conditions at Xinglong Observatory, and evaluated the feasibility for lucky imaging. Atmospheric seeing is acquired by Differential Image Motion Monitor (DIMM), of which the median value is 1.37″. atmospheric dispersion is obtained in four bands with ranges of 360 nm - 440 nm, 360 nm - 550 nm, 360 - 640 nm and 360 nm - 790 nm with an 80 cm telescope, and zenith angle was fixed to 59.8 °, 57.6 °, 48.1 °, 47.8 ° and 36.4 ° in each band, respectively. The results of the calculation which based on real parameters and of the measurement are consistent well with each other. Atmospheric extinction of BVRI was obtained with an 85cm telescope and skylight data obtained with Sky Quality Meter (SQM). The measured result indicates that lucky imaging with 50-115 cm telescope is fit for Xinglong Observatory at clear night in good seeing, and that atmospheric dispersion corrector is needed for observations. It also indicates that observation with long-wave is beneficial to decrease atmospheric dispersion and extinction and increase efficiency.**

Keywords-lucky imaging; high resolution imaging; atmospheric turbulence; atmospheric dispersion

I. INTRODUCTION

The performances of ground-base telescope are often limited by atmospheric scattering, absorption, refraction and turbulence, and the effects are not only a function of the meteorological conditions but also of wavelength. Atmospheric turbulence and dispersion can decrease spatial resolution of image, and meanwhile atmospheric extinction and skylight can reduce the SNR of data. Lucky imaging is an entirely passive technique, which acquires large number of object images with short exposure, and then best images are selected and co-added to get high resolution image. This method is a cheaper alternative to Adaptive Optics, with a lower demand on the presence of reference stars. Lucky imaging is widely used in both astronomical research [1,2,3,4,5] and high resolution imaging of space objects[6,7,8].

Xinglong Observatory of the National Astronomical Observatories, Chinese Academy of Sciences, is located at 117°34′39″ East, 40°23′26″ North, at an altitude of about 900 m. It is the largest optical observatory in China which contains several 1m class telescopes with good performance.This observatory support a series of research of lucky imaging, such as observation of crowd fields to distinguish close binaries, searching exoplanets by microlensing.

It is unlike for atmospheric conditions at different observatory, therefore we measured the atmospheric turbulence, dispersion, extinction and skylight of Xinglong Observatory, and analysis the effects for lucky imaging and the applicable condition in this paper. It provides some references for research in lucky imaging. In Sect. 2 we analysis the effects of seeing. In Sect. 3 we describe the effect of atmospheric dispersion. In Sect. 4 we describe the effects of other conditions. Finally, in Sect. 5 a summary of our discussions is given.

II. ATMOSPHERIC TURBULENCE

The atmospheric turbulence can influence the images on short time-scales, thus there are rapid variations in the image quality of the frames [9]. It is prossible that the image is diffraction limited, if the instantaneous wave-front distortion over the aperture was negligible. And Fried find that probability of obtaining a good short-exposure image, *P*, can express as follow [10]:

$$P = 5.6\exp[-0.1557(D/r_0)^2],\ D/r_0 \geq 3.5 \quad (1)$$

where D is the aperture diameter and is the coherence length of the distorted wavefront [11]. The curve of *P* varying versus to D/r_0 is drawn in figure 1. If we expect the probability better than 1%, according to formula (1), the ratio D/r_0 need smaller than 6.3.

Atmospheric seeing mirrors the intensity of atmospheric turbulence, and is usually measured with DIMM. Figure 2 shows that seeing distribution during 2010-2012 recording on a public roof at Xinglong Observatory, with the mean value 1.37″ .

The seeing is dependent upon observing wavelength(λ) through the relation [12]

$$Seeing = 0.98\frac{\lambda}{r_0} \quad (2)$$

The function describes that the longer the wavelength is, the longer the coherence length. Astronomers usually quote a reference wavelength of 500nm for using a general metric of seeing conditions [13]. And, we can include the coherence length from measured seeing according to formula (2).

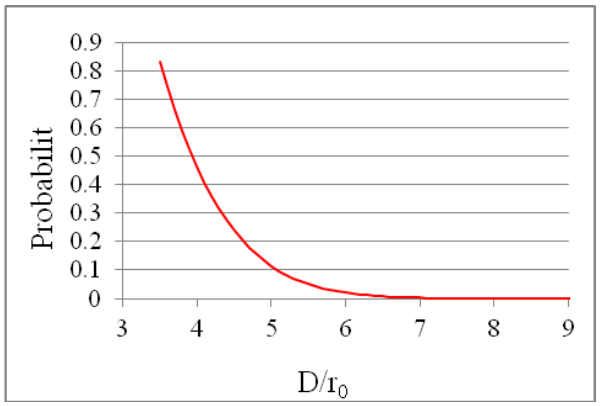

Figure 1. Probability of lucky image versus to $D/r_{0.}$

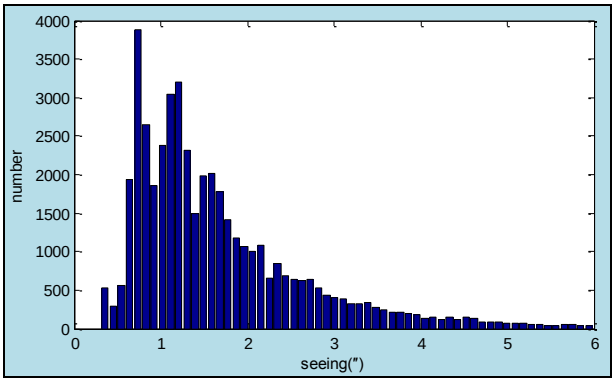

Figure 2. Seeing distribution at Xinglong Observatory.

As mentioned before, there is a probability of obtaining good short-exposure images, when exposure time is less than the atmospheric coherence time which describes the speed at which the atmospheric phase disturbances and corresponding speckle patterns evolve [13]. The relevant formulation is likely most to lucky imaging as follow:

$$\tau \propto \frac{r_0}{\Delta v} \tag{3}$$

TABLE I. SUITABLE TELESCOPE APERTURE FOR LUCKY IMAGING AT DIFFERENT BAND TABLE TYPE STYLES

Wavelength / Seeing(")	550nm(V)	640nm(R)	900nm(I)
1.00	70 cm	82 cm	115 cm
1.37	51 cm	59 cm	84 cm

where Δv is the mean velocity dispersion for the turbulent layers, and is typically of the order 10ms [14]. To keep the high spatial resolution information present in the instantaneous PSF, the length of the short exposures must be of the same order as this atmospheric coherence time. Lucky imaging is often used in observation in the night with good seeing. we can calculate suitable telescope aperture which is listed in Table I for lucky imaging at different band according to formula (1). Thus 50-115 cm telescope is suitable for lucky imaging

III. ATMOSPHERIC DISPERSION

Rays of different wavelength traversing in the same atmospheric path will suffer optical path length distortions proportional to the refractivity of air at the respective wavelengths [15]. And it will, in general, traverse in different atmospheric paths and, therefore, suffer randomly different optical path length distortions [15]. This phenomenon is called atmospheric dispersion, which is various with atmospheric temperature, humidity, pressure, altitude, and zenith angle (ZA) and wavelength. And usually humidity is considered ignorable [16].

Several area of large zenith angle was observed with 80cm telescope on 12th, Dec., 2014, and 1st, Jan., 2016 [17]. The atmospheric dispersion was calculated according to difference of stellar center positions which are obtained from the observational data in the UBVRI bands with PSF fitting with IRAF [18] software. The results are listed in Table II.

TABLE II. ATMOSPHERIC DISPERSION OF DIFFERENT WAVELENGTH

Region RA(h:m:s) DEC(°:':")	**ZA**	**360-440nm (")**	**360-550nm (")**	**360-640 nm (")**	**360-790nm (")**
01:00:36 +09:56:49	59.8 °W	1.55(0.34)	2.26(0.56)	2.76(0.32)	3.35(0.41)
07:30:16 +06:01:11	57.6 °E	1.29(0.12)	1.83(0.35)	2.41(0.30)	2.87(0.20)
02:00:00 +17:04:00	48.1 °W	1.06(0.11)	1.52(0.05)	2.01(0.04)	2.02(0.30)
04:00:20 +04:57:52	47.8 °W	0.92(0.19)	1.35(0.20)	1.59(0.16)	2.17(0.23)
08:00:45 +14:53:35	36.4 °E	0.60(0.20)	0.94(0.11)	1.23(0.28)	1.51(0.41)
07:42:06 +40 26 43	2.4 °W	-	-	-	0.12(0.28)

Table II shows the atmospheric dispersion values with different zenith angles and different bands. The first two columns give the position of observational region, and the last four give the results in bands of 360 -440nm, 360-550nm, 360-640 nm, 360-790nm. The atmospheric dispersion enhances with the increase of ZA angle and of range of wavelength, respectively. The value in brackets is relevant standard deviation.

Theoretically, the formula for approximate calculation of atmospheric refraction[19] is,

$$\rho = z' - z \approx 206265(n_\lambda - 1)\tan z \tag{4}$$

where z′ and z is the apparent and real zenith angle separately, n_λ is the atmospheric refraction index. And atmospheric dispersion is defined as,

$$\Delta\rho = \rho_1 - \rho_2 \approx 206265(n_{\lambda_1} - n_{\lambda_2})\tan z \tag{5}$$

where ρ_1 and ρ_2 is the atmospheric refraction in different wavelength, λ_1, λ_2.

There are four common models of atmospheric refraction: Elden's model [20], Rank's model [21], Owens's model [22] and simple model [23]. The results of them have slight difference, thus we choose one model to calculate [16] as follow,

Elden's model:

$$n = 1 + 0.379 \bullet 7.5 \times 10^{-3} p \bullet \frac{\left[1 + 7.5p(0.817 - 0.0133t) \times 10^{-9}\right]}{t + 273.15} \bullet (83.4213 + \frac{24060.3}{130 - \lambda^{-2}} + \frac{159.97}{38.9 - \lambda^{-2}}) \times 10^{-6} \quad (6)$$

where p is pressure in Pascal, t is temperature in Centigrade, and λ is wavelength in Micron.

Table III shows that the results of theoretical calculation of same atmospheric conditions of observation. These values is consistent with our observation listed in Table II.

TABLE III. THEORETICAL CALCULATION OF ATMOSPHERIC DISPERSION OF DIFFERENT WAVELENGTH

ZA	360-440nm(″)	360-550nm(″)	360-640 nm(″)	360-790nm(″)
59.8 °	1.54	2.62	3.11	3.58
57.6 °	1.42	2.41	2.85	3.28
48.1 °	1.00	1.70	2.02	2.32
47.8 °	0.99	1.68	2.00	2.30
36.4 °	0.66	1.13	1.34	1.54
2.4 °	-	-	-	0.09

While zenith angle is greater than 36 °, the dispersion value is more than 1.5″ in 360-790nm and more than 0.4″ in 550-790nm which is the diffraction limit of 50cm telescope. It severely impact image quality at larger zenith angle for lucky imaging. In order to do research with lucky imaging, we should take steps to compensate the effect of atmospheric dispersion. And the most effective method is to attach correctors for observation. If there is absence of corrector, it was still a good choose that observed in longer wavelength or narrow band.

IV. OTHER ATMOSPHERIC MEASUREMENT

A. Atmospheric Extinction

Atmospheric scattering and absorption can weaken the spherical radiation intensity, and change the radiation spectrum and color index. These phenomena are characterized as atmospheric extinction [24]. The atmospheric extinction coefficient is notable for observatory, which can decrease the detection limit of observational system. Only after photometric results was corrected to standard magnitude outside of atmosphere, can these data compared with other observation. Thus astronomers developed many ways to measure atmospheric extinction [25]. This article observed several standard stars at different zenith angle to obtain atmospheric extinction.

28 stars of 16 areas in landolt standard catalog from 10 to 15 magnitude at the northern hemisphere [26] are observed in the photometric night with 85cm telescope, 18th, Sep., 2014. After bias and flat correct, we got the instrumental magnitude of all bands, and calculated the atmospheric extinction index of four bands, transfer coefficient and zero-point of instrument by least square method using formula (7-10) as follow,

$$m_B = M_B + \kappa_B \cdot Airmass + \beta_B \cdot color_{B-V} + C_B \quad (7)$$

$$m_V = M_V + \kappa_V \cdot Airmass + \beta_V \cdot color_{B-V} + C_V \quad (8)$$

$$m_R = M_R + \kappa_R \cdot Airmass + \beta_R \cdot color_{V-R} + C_R \quad (9)$$

$$m_I = M_I + \kappa_I \cdot Airmass + \beta_I \cdot color_{V-I} + C_I \quad (10)$$

where m is apparent magnitude, M is catalog magnitude, κ is atmospheric extinction index, β is transfer coefficient of instrument, color is color index of standard stars, C is zero-point of instrument, and subscript of BVRI indicated which bands is.

TABLE IV. ATMOSPHERIC EXTINCTION INDEX OF XINGLONG OBSERVATION

DATE	Atmospheric extinction coefficient			
	κ_B	κ_V	κ_R	κ_I
1989.10	0.31	0.22	0.14	0.10
1995.10	0.35	0.20	0.19	0.16
1996.04	0.36	0.19	-	-
2006.09.21	0.52	0.41	0.33	0.26
2006.12.21	0.36	0.20	0.15	0.10
2014.09.18	**0.42**	**0.29**	**0.19**	**0.11**

Note：Historic data of Xinglong Observatory during year of 1989 to 2006, the last line is our result.

Table IV shows five historic results[27] and our result, and indicates that atmospheric extinction index changes with atmospheric humidity at same station. We found that the values in line 4 were larger than others caused by humidity, and that extinction of B band is larger than I band. When we observed at zenith angle of 60 °, the object had a 0.84^m lower in B band because of the extinction, which means that intensity is reduced to half. Atmospheric extinction causes the SNR decreased, and also depresses the detection limit of lucky imaging system. Thus we should observe brighter objects with longer wavelength at low humidity clear night to confront extinction.

B. Skylight

Skylight is consist with atmospheric radiation, scattering of star, moonlight, and light pollution of near cities. For long-term monitoring the various of skylight, we installed an automatic monitoring system (SQM) of skylight which pointing to south of zenith at Xinglong Observation. The SQM is developed by the Unihedron company, which can measure the skylight in magnitudes per square arcsecond, and its data are sampled every five minutes[28]. We characterize the data between 20:30 in the night and 3:30 in the morning from 2012 to 2014, presented in Figure 3. It shows that the brightness of skylight is periodic various

monthly with moon phase at range of 16-22^{m}, and that the data from June to August is different from others, which is caused by wet-season. Skylight at moonlight can depress the detection limit of lucky imaging system, so we observed at dark night or gray night.

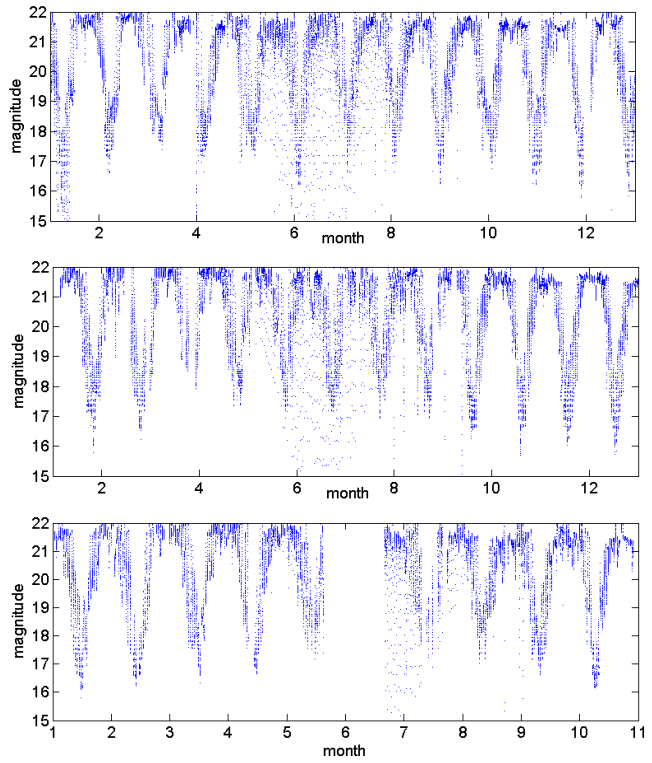

Figure 3. Skylight of 2012, 2013 and 2014 at Xinglong Observatory.

Note: there is lack of data because of stopping operating owing to the measuring equipment failure. (Figure 3 is replaced by new pictures with bigger and clear words.)

V. CONCLUSION

We measured atmospheric conditions at Xinglong Observatory, including seeing, atmospheric dispersion, atmospheric extinction and skylight, and analyzed the applicability for lucky imaging. Xinglong Observatory is suitable to choose 50-115cm telescope to do research with lucky imaging attached atmospheric dispersion corrector. And we developed lucky imaging system on 50cm telescope, and got sharp images of lunar surface, high resolution of 0.6″ of close binary and global clusters, which is two times better than traditional observation[29]. In the next step, we will do research with lucky imaging on larger telescope attached active optical system, and its atmospheric effect is much more serious to consider.

ACKNOWLEDGMENT

We thank professor Jiang Xiaojun's team for the supports at Xinglong Observatory. And our investigation is supported by funding from the National Natural Science Foundation of China through grant NSFC 11403063.

REFERENCES

[1] F. Hormuth, W. Brandner, S. Hippler, M. Janson, and T. Henning. Direct imaging of the young spectroscopic binary HD 160934[J]. Astronomy and Astrophysics, 2007, 463(2):707-711

[2] C. Ginski, M. Mugrauer, M. Seeliger, and T. Eisenbeiss. A lucky imaging multiplicity study of exoplanet host stars[J]. Mon. Not. R. Astron. Soc.,2012, 421(3): 2498-2509

[3] J. Lillo-Box, D. Barrado, and H. Bouy. High-resolution imaging of Kepler planet host candidates. A comprehensive comparison of different techniques[J]. Astronomy & Astrophysics, 2014, 566(A103): 32 pp

[4] F. M. Rica, R. Barrena, G. Vázquez, J. A. Henríquez, and F. Hernández. Orbit determination of close binary systems using lucky imaging[J]. Mon. Not. R. Astron. Soc.,2012, 419(1): 197-210

[5] N. Kains, D. M. Bramich, R. F. Jaimes, and J. Skottfelt. LIMBO: A time-series Lucky Imaging survey of variability in Galactic globular clusters[J]. Precision Asteroseismology, Proceedings of the International Astronomical Union, IAU Symposium, 2014, 301: 435-436

[6] Z. Yang, Y. Liang, H. Hu, J. Shi, C. Ren, and Q. Yu. Theoretical and experimental research of lucky imaging technique about extended objects[J]. Laser & Optoelectronics Progress, 2010, 47(5): 51004

[7] Z. Yang, J. Li, and W. Yang. High-resolution wide-area imaging of natural targets with lucky imaging technique[J]. Infrared and Laser Engineering, 2012, 41(7): 1821-1825.

[8] S. Zhang, J. Zhao, and J. Wang. An Efficient Lucky Imaging System for Astronomical Image Restoration[C]. Ryan S, The Maui Economic Development Board, Proceedings of the Advanced Maui Optical and Space Surveillance Technologies Conference, Wailea, Maui, Hawaii, 2011

[9] M. N. Law, S. T. Hodgkin, and C. D. Mackay. Discovery of five very low mass close binaries, resolved in the visible with lucky imaging[J]. Mon. Not. R. Astron. Soc.,2006, 368: 1917–1924

[10] D. L. Fried. Probability of getting a lucky short-exposure image through turbulence[J]. Optical Society of America, 1978, 68: 1651-1658

[11] D. L. Fried. Optical Resolution Through a Randomly Inhomogeneous Medium for Very Long and Very Short Exposures [J]. J. Opt. Soc. Am., 1966, 56(10): 1372-1379

[12] A. Tokovinin. From differential image motion to seeing[J], Publications of the Astronomical Society of the Pacific, 2002, 114(800): 1156-1166

[13] T. D. Staley. Lucky imaging: beyond binary stars[D]. Cambridge University, UK, 2012

[14] B. Lopez, and M. Sarazin. The ESO atmospheric temporal coherence monitor dedicated to high angular resolution imaging[J], Astronomy & Astrophysics, 1993, 276: 320-326

[15] D. Dainis, L. Lennart, M. Eva. Atmospheric Intensity Scintillation of Stars. II. Dependence on Optical wavelength[J]. Publications of the Astronomical Society of the Pacific, 1997, 109:725-737

[16] X. Zhang, and W. Jiang. Numerical calculation and results analysis for atmospheric refraction and atmospheric dispersion[J]. Opto-Electronic Engineering. 2002, 29(2): 1-5, 34

[17] E Xiang, H. Wang, K. Xu,. X. Jiang. Experimental study of atmospheric dispersion at Xinglong[J]. Infrared and laser engineering, 2017, 45(4): 244-249

[18] http://iraf.noao.edu/

[19] H. Yan, Y. Fu, and Z. Hong. An introduction of modern atmospheric refraction [M]. Shanghai: Shanghai Scintific and Technological Education Publishing House, 2006

[20] C. Lucchini, J. Gaignebet, and J. Hatat. Validation of Two Color Laser Ranging — Comparison Between: Index Integrated on the Trajectory and Index at the Station[A]. Ninth International Workshop on Laser Ranging Instrumentation, Vol. 2[C]. Canberra: Australian Government Publishing Service, 1996.628-634.

[21] D. E. Gray. American Institute of Physics Handbook:2nd ed.[M]. New York: McGraw-Hill Book Company, 1963.

[22] J. C. Owens. Optical Refractive Index of Air: Dependence on Pressure, Temperature and composition[J]. Applied Optics, 1967, 6(1):51-59.

[23] Z. Wang. Optical technology manuals(top volume)[M].Beijing: China Machine Press, 1987

[24] Y. Huang, A. Xu, and Y. Tang. Observational Astrophysics [M]. The science Publishing Company, 1984

[25] E Xiang. Application of Lucky Imaging Technology in Astronomical Observation[D]. Beijing: National astronomical observatories, Chinese academy of sciences. 2015: 28

[26] A. U. Landolt. UBVRI Photometric Standard Stars around the sky at +50 deg declination[J], The Astronomical Journal, 2013, 146:131 (41pp)

[27] W. Zheng, Y. Qiu, J. Wang, J. Deng, and J. Wei. Characterization of Xinglong 80cm TNT for Photometry[J]. Astronomical Research & Technology, 2009, 6(2):136-141

[28] J. Zhang, L. Ge, X. Lu,. Z. Cao, X. Chen, and Y. Mao. Astronomical observing conditions at Xinglong Observatory from 2007 to 2014[J]. Publications of the Astronomical Society of the Pacific, 2015, 127: 1292-1306

[29] E Xiang, X. Lu, and X. Jiang. Lucky Imaging System on the 50cm Telescope at Xinglong Observatory[J]. Infrared and Laser Engineering, 2015, 44(4): 1278-1283.